An acoustic Maxwell's fish-eye lens based on gradient-index metamaterials*

Bao-guo Yuan(袁保国)[1,2], Ye Tian(田野)[1], Ying Cheng(程营)[1,3,†], and Xiao-jun Liu(刘晓峻)[1,3,‡]

[1] *Key Laboratory of Modern Acoustics, Nanjing University, Nanjing* 210093, *China*
[2] *Department of Physics, Faculty of Science, Jiangsu University, Zhenjiang* 212013, *China*
[3] *State Key Laboratory of Acoustics, Chinese Academy of Sciences, Beijing* 100190, *China*

(Received 18 February 2016; revised manuscript received 27 June 2016; published online 25 September 2016)

We have proposed a two-dimensional acoustic Maxwell's fish-eye lens by using the gradient-index metamaterials with space-coiling units. By adjusting the structural parameters of the units, the refractive index can be gradually varied, which is key role to design the acoustic fish-eye lens. As predicted by ray trajectories on a virtual sphere, the proposed lens has the capability to focus the acoustic wave irradiated from a point source at the surface of the lens on the diametrically opposite side of the lens. The broadband and low loss performance is further demonstrated for the lens. The proposed acoustic fish-eye lens is expected to have the potential applications in directional acoustic coupler or coherent ultrasonic imaging.

Keywords: gradient index, Maxwell's fish-eye, acoustic lens, broadband

PACS: 43.20.+g, 43.20.Dk, 43.20.Bi **DOI:** 10.1088/1674-1056/25/10/104301

1. Introduction

Acoustic gradient index (GRIN) media in which the refractive index can be varied from point to point have received intensive interest for its significant applications in ultrasonic medical instruments, secret communication, acoustic detection, etc.[1–4] Rather than the conventional material, acoustic GRIN media show a spatial variation of the refraction index and then could flexibly manipulate acoustic wave in a variety of circumstances. Although acoustic GRIN media have significant potential advantages, they are far less prevalent in practical applications due to the fact that there are still challenges in the practice fabrication. Recent advances in acoustic metamaterials have promised a way to realize unusual material parameters unavailable in nature, giving the possibility in designing novel devices such as acoustic cloak,[5–7] superlens,[8–10] hyperlens,[11,12] and GRIN lens.[13–21] For example, it has been demonstrated that a metamaterial-based acoustic GRIN lens could modify sound radiation patterns with a deep-subwavelength thickness range.[14] Based on tapered labyrinthine metamaterials, Xie *et al*. also experimentally demonstrated an acoustic metasurface capable of general wavefront modulation.[15]

Among different GRIN devices with fascinating features, an optical Maxwell's fish-eye (MFE) lens is of special interest, in which a gradient of decreasing refractive index is radially out from the lens center and a point source located at the edge of the lens can be focused on the diametrically opposite side.[22,23] Recently, Liu *et al*. have implemented an optical MFE lens with an ideal index gradient based on a two-dimensional (2D) inhomogeneous artificial dielectric medium.[24] A thickness-variations-based MFE lens for flexural wave in a thin plate has been further proposed and demonstrated by simulations.[25] Subsequently, Lefebvre *et al*. experimentally demonstrated the MFE lens for flexural wave based on a thin duraluminium plate with varying thickness.[26] It would be of interest to generalize the concept of the MFE lens to acoustic wave, which may offer opportunities in application in directional acoustic coupler or coherent ultrasonic imaging.

In this paper, we have proposed a 2D acoustic Maxwell's fish-eye (AMFE) lens by using the space-coiling acoustic metamaterials (SAM) with a radius-dependent gradient refractive index. The numerical results show that the proposed lens can successfully function as an AMFE lens and has the capability to image the acoustic wave irradiated from a point source located at its surface to the diametrically opposite side of the lens. The broadband and low loss performance of the lens is further demonstrated.

2. Results and discussion

The conventional 2D AMFE lens can be shown by a cylindrical lens of a radius R, in which the refraction index varies according to the corresponding spatial position, $n = 2/[1 + (r/R)^2]$, $(0 \le r \le R)$, where r is the distance from the observing point to the lens center. Figure 1 shows the il-

*Project supported by the National Basic Research Program of China (Grant No. 2012CB921504), the National Natural Science Foundation of China (Grant Nos. 11574148, 11474162, 1274171, 11674172, and 11674175), and the Specialized Research Fund for the Doctoral Program of Higher Education, China (Grant Nos. 20110091120040 and 20120091110001).

†Corresponding author. E-mail: chengying@nju.edu.cn
‡Corresponding author. E-mail: liuxiaojun@nju.edu.cn

© 2016 Chinese Physical Society and IOP Publishing Ltd

lustration on how the AMFE lens works with no aberrations in geometric acoustics, where the black point is the source while the yellow one is the image. The arrows represent the direction of the wave propagation. It is observed that the ray paths are circles inside the lens and all rays from the point source located at the edge of the lens converge at the image point diametrically opposed to the source. The AMFE lens possesses a quite remarkable focusing property and can focus an object located at different points on the outer surface.

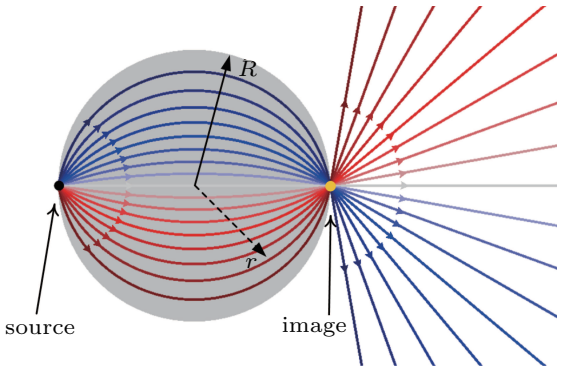


Fig. 1. (color online) Illustration on how AMFE lens works in geometric acoustics, where the black point is the source while the yellow one is the image. The arrows represent the direction of the wave propagation. R is the radius of the AMFE lens, and r is the distance from the observing point to the lens center.

We continue to realize the 2D AMFE lens by using the SAM, which has been proposed[27] and used in the design of metamaterial devices such as the GRIN lens.[18,28] Here, the SAM is adapted as the fundamental unit to compose the AMFE lens, as illustrated in Fig. 2.

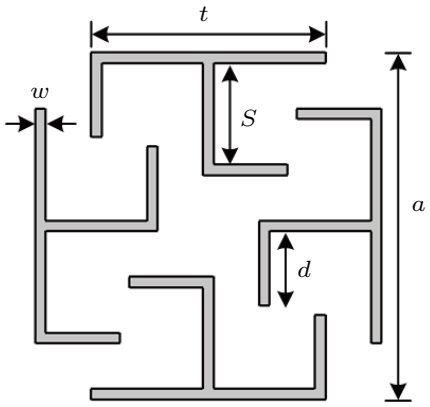


Fig. 2 Schematic diagram of the space-coiling acoustic metamaterials (SAM) unit.

At low frequency, the SAM unit can be treated as an effective medium, which can be characterized by the relative effective refractive index n_r and the relative effective acoustic impedance Z_r. n_r and Z_r can be obtained by a standard retrieval procedure.[29] Note that the scalar sound waves propagate along the zigzag channels instead of a straight line from the inlet to the outlet. Correspondingly, the propagating phase should be heavily delayed and the extent of phase delay is dependent on the SAM structure. The space is effectively coiled up and the acoustic propagation becomes effectively slow when the wave passes through the SAM. Therefore, by adjusting the structural parameters of the SAM unit, n_r can be easily modulated and then the gradually-varied refractive index that the AMFE lens needed can be flexibly obtained. It is noted that n_r should be enhanced by adding more folds into the unit. Thus the SAM may have great potential application in tunable materials.

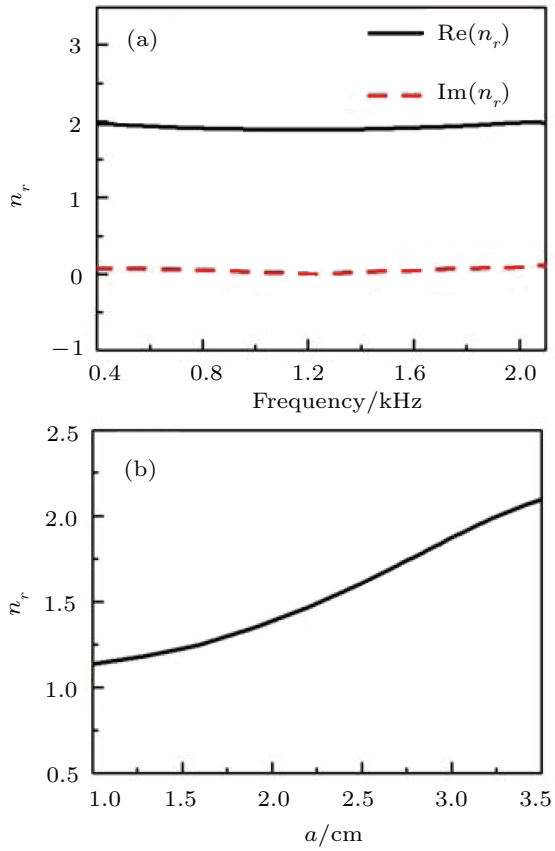


Fig. 3. (color online) (a) The real part (black solid curve) and imaginary part (red dashed curve) of the relative effective refractive index n_r as a function of frequency for the SAM unit with $w = 0.1$ cm and $a = 3.2$ cm. (b) The n_r as a function of a for the SAM unit at 2 kHz.

Figure 2 shows the SAM unit with a square cross-section structure (width a), which is constructed by immersing the identical thin epoxy resin frames (thickness w) in the background medium and forms the propagation channels of sound waves. The background medium is air. The mass density ρ_{air} and sound speed c_{air} of air are 1.21 kg/m^3 and 343 m/s, respectively, while the mass density, Young's modulus, and Poisson's ratio of epoxy resin are 1050 kg/m^3, 5.08 GPa, and 0.35, respectively. Here, the resin frames possess a thickness w of 0.1 cm to ensure the required mechanical strength against deformation in practice. For the tradeoff between n_r and the width a of the SAM unit, we choose $t = (2\times a + w)/3$, $s = (a - 4\times w)/3$, and $d = (7\times a - 19\times w)/30$, where t, s, and d are the other structural parameters of the SAM unit, as shown in Fig. 2. Then n_r can be easily tailored by appropriately selecting a. If $a = 3.2$ cm, the n_r is nearly constant at low frequency range (< 2200 Hz), as shown in Fig. 3(a). The

black solid and red dashed curves stand for the real and imaginary parts of the n_r. In addition, the imaginary part of the n_r is approximately zero, indicating the very low loss for the SAM at low frequency range. Thus, the SAM has a broad band and low loss property to design acoustic devices.

Figure 3(b) shows the variation of the n_r as a function of a at 2 kHz. It is observed that the n_r value is monotonically increased as a increases and the maximum and minimum values of the n_r are $n_{\rm rmax} \approx 2.1$ for $a = 3.5$ cm and $n_{\rm rmin} \approx 1.1$ for $a = 1$ cm in our investigation. Here, the n_r value range of SAM units is sufficient to meet the requirement to design the AMFE lens ($1 \leqslant n_r \leqslant 2$).

The desired AMFE lens has a cylindrical symmetry, where the refractive index is required to be equal at each circle with the same radius. However, due to the square profile of the SAM unit, we have to make discretization in the whole circular region and arrange the units properly according to the requirement of the refractive index. As a particular example, we choose $R = 40$ cm. In theory, the more finely the profile is discretized, the better the performance of the lens. Here, the designed lens is finally discretized in 10 rings of the SAM and hence the spacing between two neighbouring rings in the radial direction is 4 cm. Figure 4(a) shows the variation of the n_r inside the lens as a function of r. The ideal and designed values are indicated by the blue line and the red squares. It is found that the discretization by the SAM units is a good approximation to the ideal value.

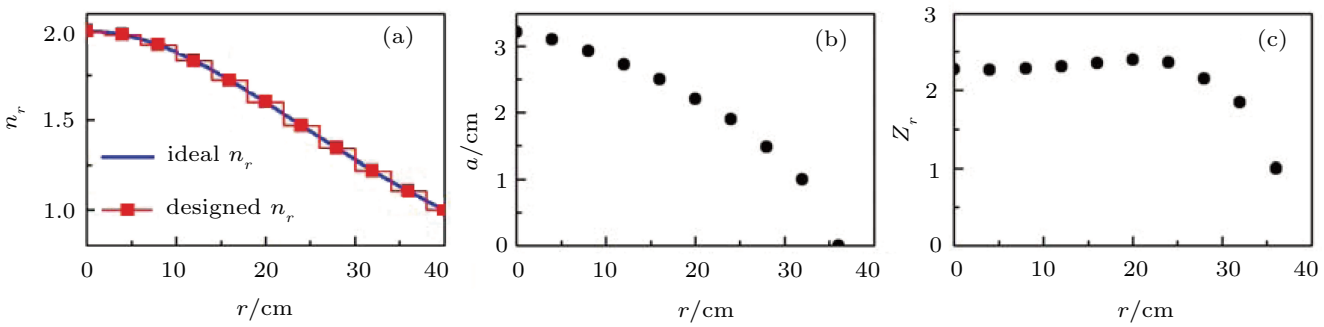


Fig. 4. (color online) (a) The variation of the n_r inside the lens as a function of r. (b) The required a-value for the AMFE lens in the radial direction. (c) The relative effective acoustic impedance Z_r for the AMFE lens with r.

Figure 4(b) shows the required a-value for the designed lens in the radial direction. The maximum value of a is 3.2 cm. We further obtain the values of the Z_r for the designed lens with r, as shown in Fig. 4(c). It is noted that the outermost annulus is empty ($a = 0$ cm) to ensure $n_r = 1$ and the impedance match with air ($Z_r = 1$). Meanwhile, it is found from Fig. 4(c) that the maximum value of the Z_r is not so large (≈ 2.4), which means that the structure proposed here can be coupled to the surrounding medium well. Thus, it is negligible for the reflection associated with impedance mismatch. According to Fig. 4(b), the proposed AMFE lens is fabricated by gradually decreasing the a-value, as shown in Fig. 5. The proposed lens is composed of a circular array of the SAM units and the total number of the units is 289.

We have further performed the full-wave simulations to describe the acoustic property of the AMFE lens by using a finite-element method. Figure 6 shows the distributions of the acoustic pressure fields around the AMFE lens when a point source irradiated in the surface of the AMFE lens at (a) 1 kHz, (b) 1.5 kHz, and (c) 2 kHz, where the solid circle indicates the boundary of the lens. As predicted, the transmitted wave is focused on the diametrically opposite side of the lens. The focusing point quite obviously locates at $x = 40$ cm and $y = 0$ cm, while the point source and the center of the lens is fixed at $x = -40$ cm, $y = 0$ cm, and $x = 0$ cm, $y = 0$ cm, respectively. In addition, the variation of frequency from 1 kHz to 2 kHz cannot affect the focusing behavior, because there is no resonant cell required in the design of the lens and the refractive index of the SAM is insensitive to the frequency of the incident acoustic waves. Thus, the designed device shows broadband and low loss. We further note that the wavefront shows flat when the wave propagates in a halfway of the lens, suggesting that a half lens would convert a point source located at the border of the lens into a plane wave and *vice versa*. Such a lens may be useful in directional acoustic coupler or coherent ultrasonic imaging.

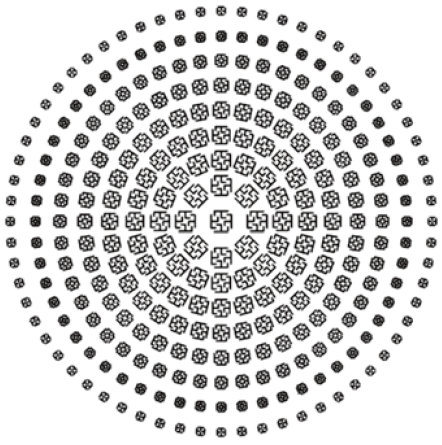


Fig. 5. Schematic view of the proposed AMFE lens. The proposed AMFE lens is fabricated by gradually decreasing the a-value, and the total number of the SAM units is 289.

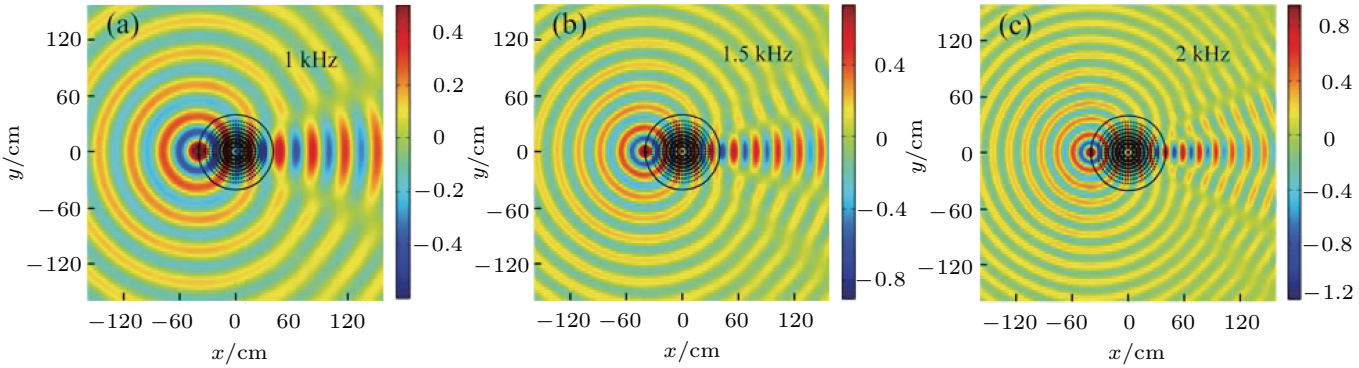


Fig. 6. (color online) Distribution of the simulated acoustic pressure fields for the AMFE lens: (a) $f = 1$ kHz, (b) $f = 1.5$ kHz, and (c) $f = 2$ kHz, in which the solid circle indicates the boundary of the lens.

We have further calculated the transverse profiles of the pressure amplitude passing through the focal spot at $x = 40$ cm for the designed AMFE lens with different frequencies, as shown in Fig. 7. The dashed-dotted, dashed and solid curves represent for that at the frequencies of 1, 1.5, and 2 kHz, respectively. For comparison, the profile at each frequency is normalized to the peak value. At 2 kHz, the AMFE lens shows a good focal spot with a full-width at half maximum (FWHM) of 14 cm, while the FWHM at 1 kHz and 1.5 kHz are 32 cm and 20 cm, respectively. Thus, the focusing capability may be better at higher frequency.

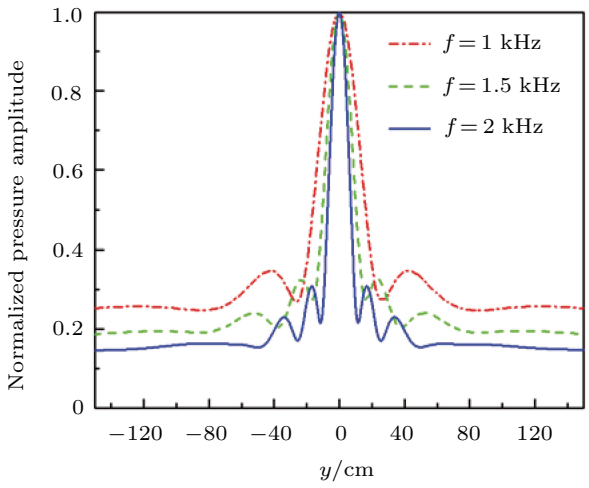


Fig. 7. (color online) Normalized pressure amplitudes passing through the focal spot for the AMFE lens with different frequencies at 1 kHz, 1.5 kHz, and 2 kHz.

3. Conclusion

We have proposed a two-dimensional acoustic Maxwell's fish-eye lens based on the space-coiling acoustic metamaterials. The gradually-varied refractive index is obtained by adjusting the structural parameters of the space-coiling acoustic units to design the lens. We further simplify the fabrication process of acoustic Maxwell's fish-eye lens. The proposed lens has the capability to focus the acoustic wave irradiated from a point source at the surface of the lens on the diametrically opposite side of the lens. The broadband and low loss performance of the lens is further confirmed. The proposed acoustic fish-eye lens is expected to have the potential applications in directional acoustic coupler or coherent ultrasonic imaging.

References

[1] Climente A, Torrent D and Sánchez-Dehesa J 2010 *Appl. Phys. Lett.* **97** 104103
[2] Lin S C S, Huang T J, Sun J H and Wu T T 2009 *Phys. Rev. B* **79** 094302
[3] Martin T P, Layman C N, Moore K M and Orris G J 2012 *Phys. Rev. B* **85** 161103
[4] Peng S S, He Z J, Jia H, Zhang A Q, Qiu C Y, Ke M Z and Liu Z Y 2010 *Appl. Phys. Lett.* **96** 263502
[5] Zigoneanu L, Popa B I and Cummer S A 2014 *Nat. Mater.* **13** 352
[6] Zhang S, Xia C G and Fang N 2011 *Phys. Rev. Lett.* **106** 024301
[7] Cheng Y, Yang F, Xu J Y and Liu X J 2008 *Appl. Phys. Lett.* **92** 151913
[8] Zhang S, Yin L L and Fang N 2009 *Phys. Rev. Lett.* **102** 194301
[9] Liu A P, Zhou X M, Huang G L and Hu G K 2012 *J. Acoust. Soc. Am.* **132** 2800
[10] Zhu J, Christensen J, Jung J, Martin-Moreno L, Yin X, Fok L, Zhang X and Garcia-Vidal F J 2011 *Nat. Phys.* **7** 52
[11] Li J S, Fok L, Yin X B, Bartal G and Zhang X 2009 *Nat. Mater.* **8** 931
[12] Gu Y, Cheng Y and Liu X J 2015 *Appl. Phys. Lett.* **107** 133503
[13] Li D, Zigoneanu L, Popa B I and Cummer S A 2012 *J. Acoust. Soc. Am.* **132** 2823
[14] Zigoneanu L, Popa B I and Cummer S A 2011 *Phys. Rev. B* **84** 024305
[15] Xie Y B, Wang W Q, Chen H Y, Konneker A, Popa B I and Cummer S A 2014 *Nat. Commun.* **5** 5553
[16] Chang T M, Dupont G, Enoch S and Guenneau S 2012 *New J. Phys.* **14** 035011
[17] Zhang Z, Li R Q, Liang B, Zou X Y and Cheng J C 2015 *Chin. Phys. B* **24** 024301
[18] Li Y, Liang B, Tao X, Zhu X F, Zou X Y and Cheng J C 2012 *Appl. Phys. Lett.* **101** 233508
[19] Tang K, Qiu C Y, Ke M Z, Lu J Y, Ye Y T and Liu Z Y 2014 *Sci. Rep.* **4** 6517
[20] Torrent D and Sánchez-Dehesa J 2007 *New J. Phys.* **9** 323
[21] Yuan B G, Cheng Y and Liu X J 2015 *Appl. Phys. Express* **8** 027301
[22] Maxwell J C 1854 *Camb. Dublin Math. J.* **8** 188
[23] Tai C T 1958 *Nature* **182** 1600
[24] Liu J B, Mendis R and Mittleman D M 2013 *Appl. Phys. Lett.* **103** 031104
[25] Climente A, Torrent D and Sánchez-Dehesa J 2014 *Appl. Phys. Lett.* **105** 064101
[26] Lefebvre G, Dubois M, Beauvais R, Achaoui Y, Ing R K, Guenneau S and Sebbah P 2015 *Appl. Phys. Lett.* **106** 024101
[27] Liang Z X and Li J S 2012 *Phys. Rev. Lett.* **108** 114301
[28] Li Y, Yu G K, Liang B, Zou X Y, Li G Y, Cheng S and Cheng J C 2014 *Sci. Rep.* **4** 6830
[29] Fokin V, Ambati M, Sun C and Zhang X 2007 *Phys. Rev. B* **76** 144302